J. Fluid Mech. (1986), *vol.* 167, *pp.* 415–426
Printed in Great Britain

Viscous interactions of many neutrally buoyant spheres in Poiseuille flow

By JEFFREY A. SCHONBERG, DONALD A. DREW AND GEORGES BELFORT

Department of Chemical Engineering and Environmental Engineering *and* Department of Mathematical Sciences, Rensselaer Polytechnic Institute, Troy, NY 12180, USA

(Received 25 June 1984 and in revised form 12 November 1985)

A theory is developed to predict the motion of N neutrally buoyant spheres suspended in laminar flow between parallel plates. The spheres are at large separation yet nearer each other than the duct walls, and the Reynolds number is small. In this parameter range, viscous interactions are larger than inertial effects, and can be represented in terms of a superposition of 'strainlets'. Several examples are given to show this viscous interaction effect. Near the leading edge of a front of spheres or near the trailing edge significant lateral migration velocities can occur, being at least one order of magnitude larger than inertially induced migration velocities. This phenomenon may have a negative effect on 'chromatographic' separation schemes, affecting particle concentration, recovery and resolution.

1. Introduction

The motion of small particles in a viscous medium in which the particle number per unit volume (concentration) varies from dilute to concentrated suspensions is found in a wide variety of processes. Examples include (O'Neill 1981): suspension and polymer rheology (Russel 1981), continuum mechanics (Drew 1983), and diffusional transport processes in suspensions of Brownian particles, erythrocyte motion in capillary blood flow, gel permeation chromatography, field flow fractionation, flow of fibre suspensions in papermaking processes and of latex particles in emulsion based paints, cross-flow filtration of concentrated suspensions, ferro-fluid rheology, shear-gradient coagulation in hydrosols, emulsification mechanisms in colloid mills and the motion of suspended rock crystals in molten rocks.

Since Stokes' celebrated work (Stokes 1851) on the motion of particles in viscous flow at small Reynolds numbers, a plethora of studies has appeared in the literature. New developments and extensions have accounted for such effects as particle rotation, non-spherical geometry, inertial effects, wall effects, particle–particle interactions, density effects, liquid droplets and gas bubbles, and the inclusion of electrical and magnetic forces acting on the particles (Batchelor 1976).

Of specific interest here is the motion and behaviour of neutrally buoyant solid spherical particles suspended in laminar flow moving in a non-porous duct under near-creeping-flow conditions. Although the Reynolds number of the bulk flow can never be exactly zero, the relative importance of viscous versus inertial effects for low-Reynolds-number hydrodynamics is of interest in the creeping-flow limit. Various researchers (Ho & Leal 1974; Vasseur & Cox 1976; Ishii & Hasimoto 1980; and Altena & Belfort 1984) have solved the integral equations (Cox & Brenner 1968) for the inertially induced lateral migration of single neutrally buoyant particles moving in Poiseuille flow in non-porous and porous ducts. Although 'asymmetric' migration for the sedimentation of interacting particles has been analysed (Hocking 1964; Bretherton 1964) and measured (Koglin 1971), the lateral migration of interacting Stokesian particles moving in a homogeneous but bounded Poiseuille flow has not. The reasons for addressing this question are (1) to obtain an estimate of the size of the viscous effects and conditions under which they are important relative to the inertial effects, and (2) to lay the foundation for extending the single-particle work (Cox & Brenner 1967, 1968) to three boundaries (two particles and enveloping boundary) for non-porous and porous walls (Schonberg, Drew & Belfort 1986). Previous research, focused on two-body interactions in Couette flows, has shown that these viscous effects can cause noticeable temporary lateral migrations but no net lateral movement (Eckstein, Bailey & Shapiro 1977; Goldsmith & Mason 1967).

The present paper provides a theory to predict the viscous interactions of many neutrally buoyant spheres, suspended in Poiseuille flow between flat plates. This theory shows the effects of higher concentration of particles in shear flow. The theory indicates circumstances under which net lateral migrations will occur, and is applied to a cluster of spheres straddling the centreplane of the flow. Computer experiments show that noticeable lateral migrations occur and, more importantly, that the cluster spreads axially in the flow. These movements occur even when the cluster is so structured that every particle initially sits on streamlines of equal velocity (of the undisturbed flow). This finding has implications relevant to lateral migration based chromatography schemes.

2. Statement of problem

Consider two or more neutrally buoyant spheres suspended in a fluid flowing between two parallel plates. Far from the bodies the flow field is Poiseuillean. Let the bodies be well separated and the particle Reynolds numbers small. The forces and torques on each sphere will arise from the imposed pressure gradient, the 'slip' velocity relative to the undisturbed flow, the imposed shear near each body, and correction fields due to the wall and the other bodies.

Let a be the characteristic body radius, U the scaling of the undisturbed flow (its maximum velocity) and d the channel width. Furthermore define $\kappa = a/d$ and $Re = aU/\nu$, where ν is the kinematic viscosity of the flowing liquid. Viewing the problem as a fixed laboratory observer, and requiring

$$Re \ll \kappa \tag{2.1}$$

the governing equations are approximated by the familiar Stokes equations

$$\left.\begin{aligned} \mu\nabla^2\boldsymbol{v}' - \nabla p' &= \mathbf{0}, \\ \nabla\cdot\boldsymbol{v}' &= 0, \\ \boldsymbol{v}' &\sim \boldsymbol{u}'(\boldsymbol{r}) \quad (r\rightarrow\infty), \\ \boldsymbol{v}' &= \boldsymbol{V}'_{\mathrm{A}} + \boldsymbol{\Omega}'_{\mathrm{A}}\times\boldsymbol{r}'_{\mathrm{A}} \quad \text{on body A}, \\ \boldsymbol{v}' &= \boldsymbol{V}'_{\mathrm{B}} + \boldsymbol{\Omega}'_{\mathrm{B}}\times\boldsymbol{r}'_{\mathrm{B}} \quad \text{on body B}, \\ &\text{etc.} \ldots, \\ \boldsymbol{v}' &= \mathbf{0} \quad \text{on walls}, \end{aligned}\right\} \tag{2.2}$$

where $\boldsymbol{V}'_{\mathrm{A}}$ and $\boldsymbol{\Omega}'_{\mathrm{A}}$ respectively describe the dimensional translation and rotation of body A, $\boldsymbol{r}'_{\mathrm{A}}$ is the position of any point on the surface of body A relative to its centre,

μ is the viscosity of the flowing fluid, $\boldsymbol{v}$ is the total velocity field and p the total pressure field. The quantities are subscripted according to the identity of the corresponding sphere and the prime denotes a dimensional quantity.

3. Solution by asymptotic expansion

The governing equations may be further approximated by an asymptotic expansion. The leading-order solution of (2.2) is simply the summation of the flow fields induced by the response of each sphere to the Poiseuille flow in the absence of the other spheres and the walls. Once the asymptotic behaviour of this elementary field is known, specific scaling restrictions can be developed for the distance of the spheres from each other and the nearest wall such that the leading-order solution is a good approximation. This elementary field is defined by dimensionless equations where the coordinate axes translate with the sphere but do not rotate. The position vector relative to this coordinate system is denoted by $\boldsymbol{r}$.

$$\left.\begin{aligned} \nabla^2\boldsymbol{v}-\nabla p &= \boldsymbol{0}, \\ \nabla\cdot\boldsymbol{v} &= 0, \\ \boldsymbol{v} &\sim \boldsymbol{u}(\boldsymbol{r}) \quad (r\rightarrow\infty), \\ \boldsymbol{v} &= \boldsymbol{\Omega}_{\mathrm{A}}\times\boldsymbol{r} \quad \text{on A.} \end{aligned}\right\} \tag{3.1}$$

Define a disturbance flow field

$$\left.\begin{aligned} \boldsymbol{v}^* &= \boldsymbol{v}-\boldsymbol{u}, \\ p^* &= p-P, \end{aligned}\right\} \tag{3.2}$$

where ($\boldsymbol{u}$, P) represents the laminar, undisturbed flow. Substituting (3.2) into (3.1) yields

$$\left.\begin{aligned} \nabla^2\boldsymbol{v}^*-\nabla p^* &= \boldsymbol{0}, \\ \nabla\cdot\boldsymbol{v}^* &= 0, \\ \boldsymbol{v}^* &\sim \boldsymbol{0} \quad (r\rightarrow\infty), \\ \boldsymbol{v}^* &= \boldsymbol{\Omega}_{\mathrm{A}}\times\boldsymbol{r}-\boldsymbol{u}(\boldsymbol{r}) \quad \text{on A.} \end{aligned}\right\} \tag{3.3}$$

Equations (3.3) may be solved using a polyadic-velocity and pressure-field formulation in which the response of the sphere to the undisturbed flow is a sum of polyadic functions of position, each multiplying a particular polyadic derivative of the undisturbed flow evaluated at the centre of the sphere (Brenner 1964). If the sphere is neutrally buoyant and torque-free, the sum is greatly simplified. In particular the terms associated with the slip velocity (including the Stokeslet) and the vorticity of the fluid are unimportant. The resulting expression for the velocity is

$$v_i^* = -\frac{5}{2}\frac{1}{r^5}r_i r_j r_k(e_{\mathrm{A}})_{kj}+O(r^{-4})\,O((\nabla\boldsymbol{u})_{\mathrm{A}})+O(r^{-3})\,O(\boldsymbol{u}_{\mathrm{A}})+O(r^{-3})\,O((\nabla\nabla\boldsymbol{u})_{\mathrm{A}}), \tag{3.4}$$

where $\boldsymbol{e}_{\mathrm{A}}$ is the rate of strain tensor of the undisturbed flow at A,

$$(e_{\mathrm{A}})_{ij} = \tfrac{1}{2}((\nabla_i u_j)_{\mathrm{A}}+(\nabla_j u_i)_{\mathrm{A}}), \tag{3.5}$$

and the polyadic function multiplying $\boldsymbol{e}_{\mathrm{A}}$ in the leading term of (3.4), $-\tfrac{5}{2}(r^{-5})\,r_i r_j r_k$, is defined as the strainlet. Once the elementary solution has been found, the geometric restrictions of the asymptotic expansion may be developed through the introduction of parameters and an order-of-magnitude analysis.

There are three lengthscales: a, the sphere radius; l, the characteristic interparticle distance; and d, the channel width. Define the quantities

$$\beta \equiv \frac{a}{l}, \tag{3.6}$$

$$\kappa \equiv \frac{a}{d}, \tag{3.7}$$

and the following stretched coordinates:

$$\tilde{\boldsymbol{r}} \equiv \kappa \boldsymbol{r}, \tag{3.8}$$

$$\bar{\boldsymbol{r}} \equiv \beta \boldsymbol{r}. \tag{3.9}$$

Since the undisturbed flow field varies over the width of the channel

$$(\tilde{\boldsymbol{\nabla}}\boldsymbol{u})_{\mathrm{A}} = O(1). \tag{3.10}$$

Using (3.8) we find

$$(\boldsymbol{\nabla}\boldsymbol{u})_{\mathrm{A}} = O(\kappa). \tag{3.11}$$

Similarly

$$(\boldsymbol{\nabla}\boldsymbol{\nabla}\boldsymbol{u})_{\mathrm{A}} = O(\kappa^2) \tag{3.12}$$

and from (3.8) and the force balance (Brenner 1964)

$$\boldsymbol{u}_{\mathrm{A}} = O(\kappa^2). \tag{3.13}$$

We wish to find the influence of one sphere on a second sphere and so (3.4) must be rewritten in terms of $\bar{\boldsymbol{r}}$. Therefore, using (3.9) and (3.11)–(3.13) we have

$$v_i^* = -\frac{5}{2}\frac{1}{\bar{r}^5}\bar{r}_i\bar{r}_j\bar{r}_k(\tilde{e}_{\mathrm{A}})_{jk}\,\kappa\beta^2 + O(\kappa\beta^4) + O(\kappa^2\beta^3). \tag{3.14}$$

To determine the magnitude of the wall effect, (3.14) is transformed to the $\tilde{\boldsymbol{r}}$-coordinate. Using the wall-effect analysis (Cox & Brenner 1967) we find that the wall-induced disturbance velocity is $O(\kappa^3)$. Not only will the presence of the wall give rise to a term in the asymptotic expansion but the sphere nearest each sphere previously analysed in the elementary problem will induce a flow field. The neighbouring sphere is neutrally buoyant and free to rotate and thus responds to the strainlet field just as the sphere responds to the Poiseuille flow. Furthermore the induced flow field is itself a strainlet field. Thus using (3.4), (3.5) and (3.9) we find that the 'nearest-sphere' term in the asymptotic expansion is $O(\kappa\beta^5)$ in the vicinity of the central sphere.

If we require

$$\beta^2 \ll 1 \tag{3.15}$$

and

$$\kappa\beta \ll 1, \tag{3.16}$$

the smaller terms in (3.14) as well as the nearest-sphere terms may be neglected. If we require

$$\kappa^2 \ll \beta^2, \tag{3.17}$$

the wall-effect terms in the asymptotic expansion may be neglected. These criteria are not unrealistic. They would permit a value of $\beta \approx 0.1$ and $\kappa \approx 0.01$, which are quite reasonable for flowing suspensions such as pulp 'fines' or living cells in aqueous media.

This order-of-magnitude analysis has relevance to discussions of inertially induced lift. Previous researchers (Cox & Brenner 1968) have analysed the single-sphere problem for the case of

$$Re \ll \kappa \ll 1, \tag{3.18}$$

which is equivalent to that used here. They found convective acceleration effects of size $O(Re\kappa^2)$. Subsequent theoretical work for multisphere problems (Schonberg, Drew & Belfort 1986) has shown that local and convective acceleration effects are of the same size. Therefore the viscous effect discussed here for the same Reynolds-number limitation (3.18) is much larger than acceleration effects. Thus if a near-creeping-flow problem involves two or more spheres in certain configurations the complex perturbation in Reynolds number need not be done.

In conclusion (3.14) can be recast to indicate pair-wise interaction as

$$(u^*_{ij})_k = -\frac{5}{2}\frac{1}{x^5}x_k\,x_l\,x_m(\tilde{e}_j)_{ml}\,\kappa\beta^2; \quad \boldsymbol{x} \equiv \bar{\boldsymbol{r}}_{ij}, \tag{3.19}$$

where $\boldsymbol{u}^*_{ij}$ is the induced velocity on body i due to body j; $\bar{\boldsymbol{r}}_{ij}$ is the position vector of body i, relative to body j; k refers to the component in the k-direction; and $\tilde{\boldsymbol{e}}_j$ is the rate-of-strain tensor of the undisturbed flow at body j in terms of $\bar{\boldsymbol{r}}$.

4. Application to Poiseuille flow between parallel plates

Consider figure 1, which defines two coordinate systems, one fixed on the wall and a second moving amidst the spheres, with a velocity prescribed by the undisturbed flow field. Having defined the local coordinate system scaled by the interparticle distance we have

$$z_2 = z_2^0 + \frac{l}{d}y_2, \tag{4.1}$$

where z_2^0 defines the location of the origin of the local coordinates. Using (3.8) and (3.9), (4.1) can be rewritten as

$$z_2 = z_2^0 + \frac{\kappa}{\beta}y_2. \tag{4.2}$$

Substituting this into the velocity profile for Poiseuille flow yields the following expression for the undisturbed flow near the cluster:

$$\boldsymbol{u}(z) = \boldsymbol{u}(z^0) - \frac{\kappa}{\beta}y_2\,4(2z_2^0-1)\,\boldsymbol{e}_1 - 4\left(\frac{\kappa}{\beta}\right)^2 y_2^2\,\boldsymbol{e}_1 \tag{4.3}$$

and the velocity gradient as

$$\tilde{\nabla}_2\,u_1(z) = \tilde{\nabla}_2\,u_1(z^0) - 8\frac{\kappa}{\beta}y_2. \tag{4.4}$$

Using (3.19), (3.5) and (4.3) yields the interaction velocity

$$(u^*_{ij})_k = -\frac{5}{2}\frac{1}{x^5}x_k\,x_1\,x_2\left(\tilde{\nabla}_2\,u_1(z^0) - 8y_2\frac{\kappa}{\beta}\right)\kappa\beta^2. \tag{4.5}$$

In order to see effects due to the parabolic shape of the undisturbed flow we require the interaction velocity, as well as the slip velocity, to be much less than the passing velocity, calculated using (4.3); in the direction of $\boldsymbol{e}_1$. Thus we assume

$$\beta^4 \ll \kappa. \tag{4.6}$$

Note that this restriction is practically subsumed under the previous restrictions. In practice spheres may be of different size. To allow for this define

$$b_i \equiv \frac{\text{radius of sphere } i}{a} \tag{4.7}$$

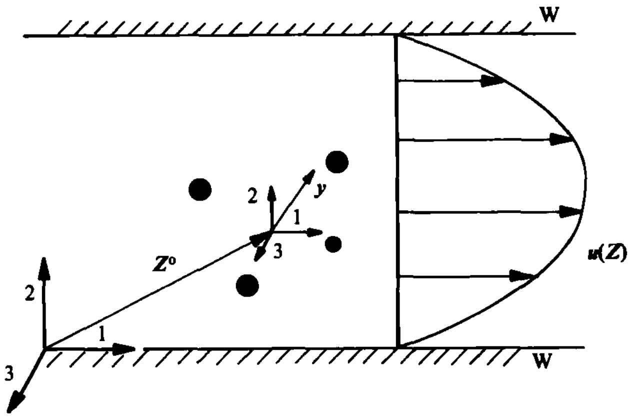

FIGURE 1. Definition of fixed and moving coordinate systems.

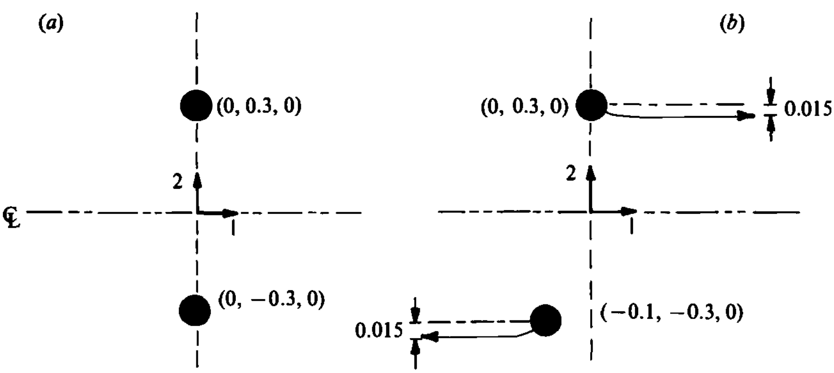

FIGURE 2. Two-body interaction near centreline of velocity profile.

where a is the radius of the median sphere. Whence (4.5) becomes

$$(u^*_{ij})_k = -\frac{5}{2}\frac{x_k x_1 x_2}{x^5}\left(\tilde{\nabla}_2 u_1(z^0) - 8\frac{\kappa}{\beta}(y_j)_2\right) b_j^3 \kappa \beta^2. \tag{4.8}$$

Trajectories of a system of particles in plane Poiseuille flow can be obtained using Euler's method, taking advantage of the linearity of the Stokes equations.

5. Results

The preceding development was implemented on an IBM 3081D computer. Computation times were very short, even for arrays of 10 spheres. All experiments were done in the $y_3 = 0$ plane. Computer experiments were first performed with two spheres. Spheres placed on streamlines of differing velocity, in terms of the undisturbed flow, had little effect on one another because they spent so little time in the same region. Spheres placed on either side of the centreline of the velocity profile in a symmetrical fashion had no effect on each other. However, if one was slightly downstream of the other the leading sphere migrated toward the centreline while the trailing sphere migrated away. The extent of these lateral migrations was limited because the leading particle moving to a region of higher velocity accelerated while the trailing particle decelerated. Therefore, the particles eventually separated,

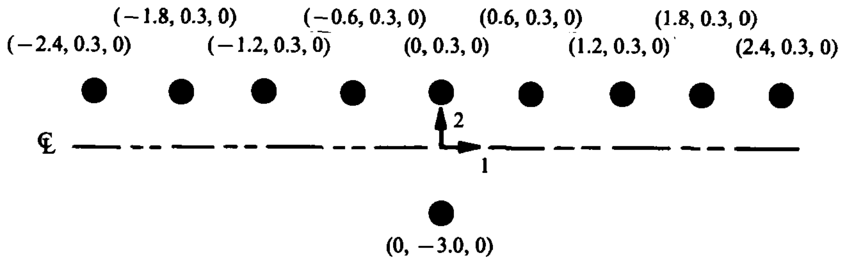

FIGURE 3. Interaction of a single sphere and a cluster, symmetric about centreline; initial position.

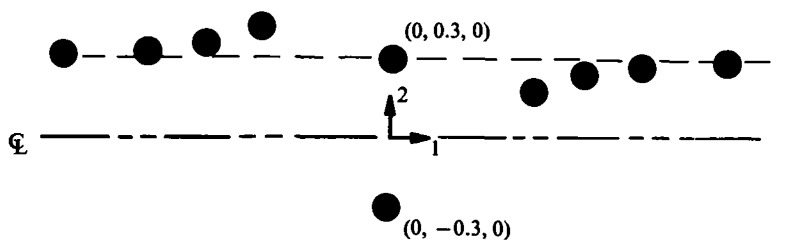

FIGURE 4. Distortion of single sphere and cluster (lateral migration exaggerated).

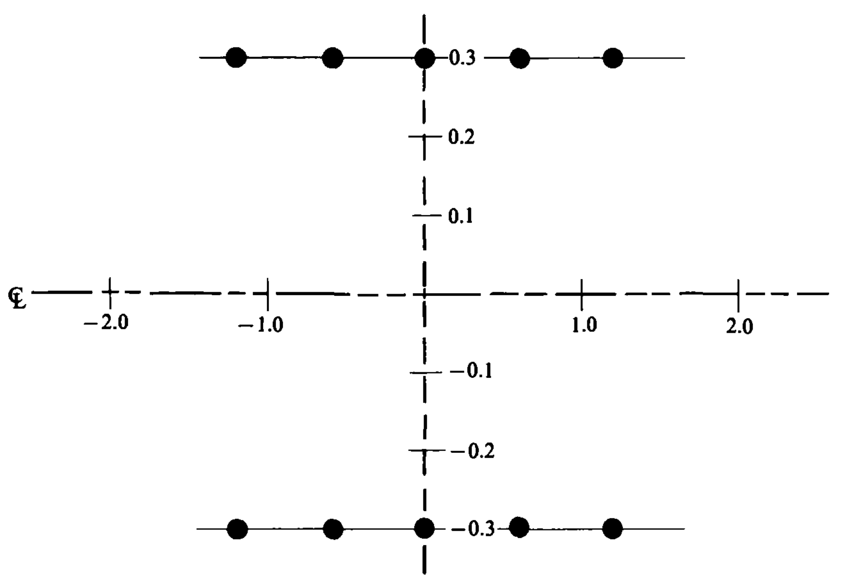

FIGURE 5. Initial position of a cluster of ten spheres straddling the centreline symmetrically (spheres not to scale).

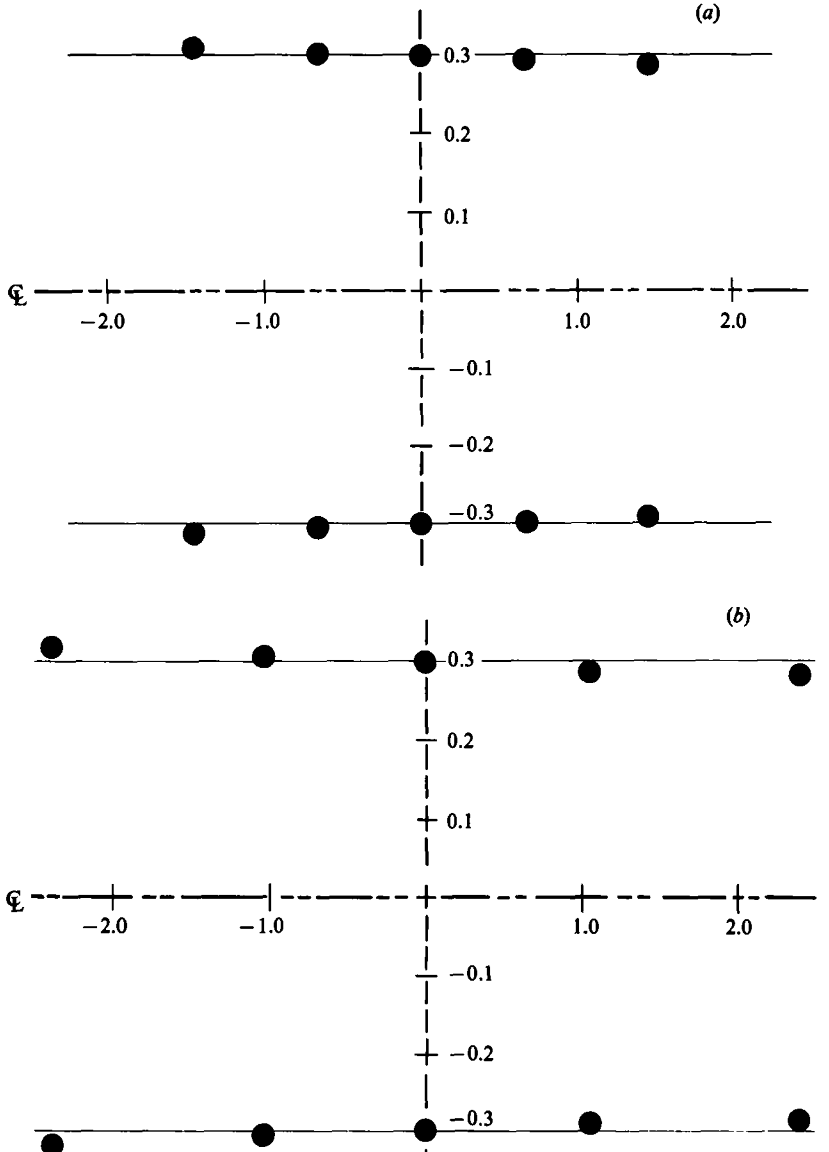

FIGURE 6. Cluster at (a) time = 600 and (b) 1400 showing migration of spheres and stretching of cluster.

sufficiently reducing significant interactions. Using $\beta = 0.05$, $\kappa = 0.01$ and placing the spheres 0.3 from the centreline, they migrated 0.015 laterally (on the interparticle distance scale) as can be seen from figure 2.

Experiments were also conducted with ten spheres of equal size. In one experiment, nine spheres were placed on one side of the centreline, all located 0.3 from the centreline and 0.6 from each other. Meanwhile, a tenth body was located 0.3 from the centreline on the other side, having the same y_1 coordinate as the fifth body in the train of nine, as shown in figure 3. The nine bodies had little net effect on the tenth while the tenth had a noticeable effect on the other nine. The four leading

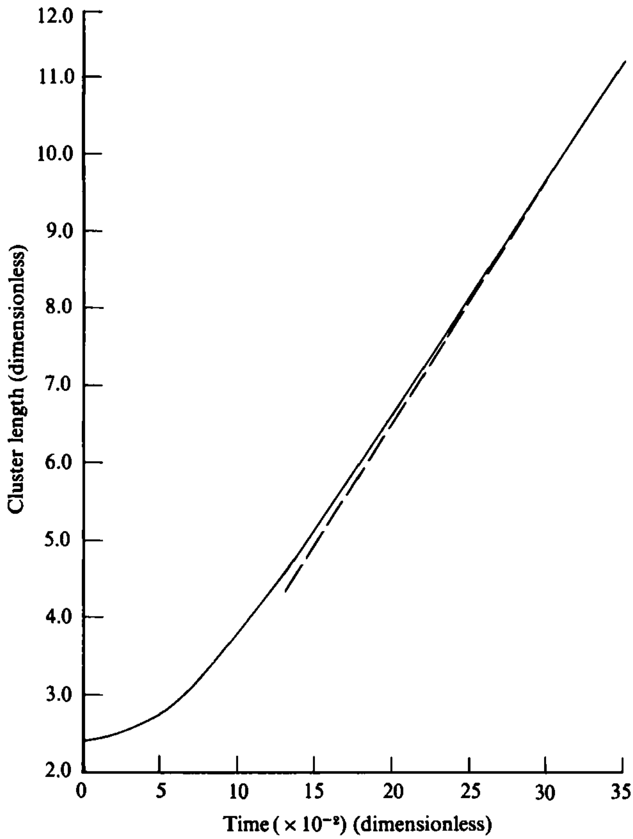

FIGURE 7. The growth of the length of the cluster shown in figure 5 with time.

spheres migrated toward the centreline, with the spheres nearer the tenth one migrating faster. Thus these nearer spheres accelerated and approached the farther leading spheres, compressing the line-up. Computation ceased when the spheres came too close, as the model requires x to be of magnitude $O(1)$. Due to this shortened computation time the lateral migrations were relatively small. The trailing spheres were similarly affected with the pattern compressing as the nearer spheres decelerated (see figure 4).

In a second experiment, five spheres were placed on each side of the centreline. The spheres were so lined up that they formed a double line of five pairs two abreast, as shown in figure 5. The leading spheres migrated inwards while the trailing spheres migrated outwards. The particle pairs remained 'in step'; however, the leading pairs accelerated downstream while the trailing pairs decelerated. Lateral migration of one of the leading spheres was nearly the same as in the two-body experiment. These dramatic results, shown in figure 6, have interesting implications. Notice from figure 7 that the 'smearing' process is at first slow but speeds up as the spheres migrate laterally. When the spheres are sufficiently separated, interactions are weakened and the 'smearing' rate settles to a constant as the only mechanism is convection by the undisturbed flow.

Finally a train of five particles was permitted to pass a second such train, on the same side of the centreline, as in figure 8. There was little effect on either train, they merely jiggled as they passed with very small amplitude and no net displacement.

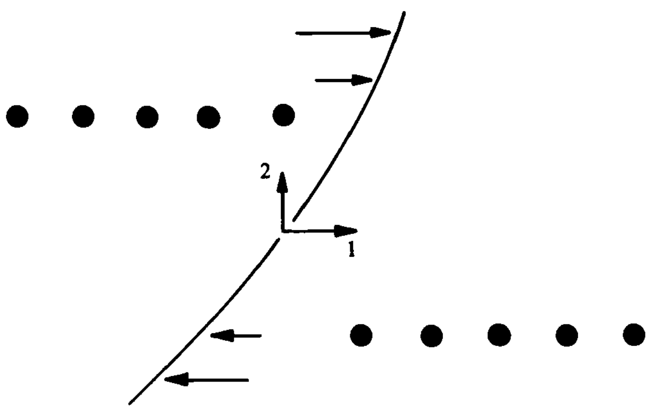

FIGURE 8. Clusters of spheres passing one another have little effect.

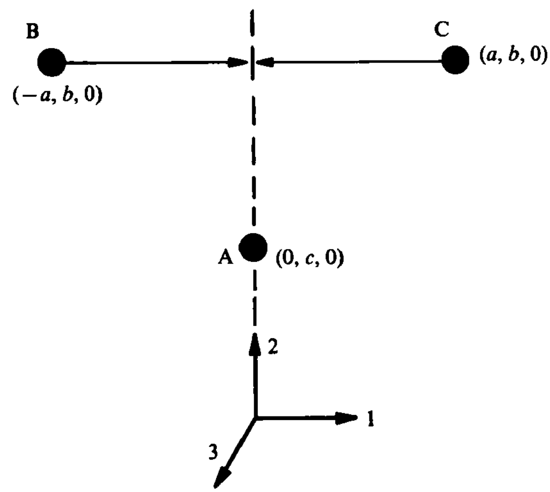

FIGURE 9. Fore–aft symmetry in a plane around body A.

6. Discussion

The results in this paper have some interesting implications for chromatographic separation processes. For large particles, where Brownian diffusion is negligible compared with advection, these findings are directly relevant to the resolution for separating solutes. For example, lateral-migration-based-chromatography schemes (Altena & Belfort 1984) rely on particles aligning along a particular or several closely spaced streamlines on either side of the centreline. Thus axial dispersion resulting from lateral migration due to viscous interactions will spread a cluster both forward and backward from the centre of mass of the cluster, effecting its particle concentration, recovery and resolution. Consider (4.8) as applied to the lateral direction, $k = 2$. Consider a sphere A being influenced by two other spheres B and C having the same y_2 values as one another but different from A. Further let the spheres be of the same size. Constrain the spheres to the $y_3 = 0$ plane and let x_1 from one sphere be $-x_1$ of the other, as shown in figure 9. Then it is clear from (4.8) that there is no net effect on sphere A. Therefore, if there is fore–aft symmetry of particle concentration in the duct, there should be no lateral force of viscous origin on any single sphere. In

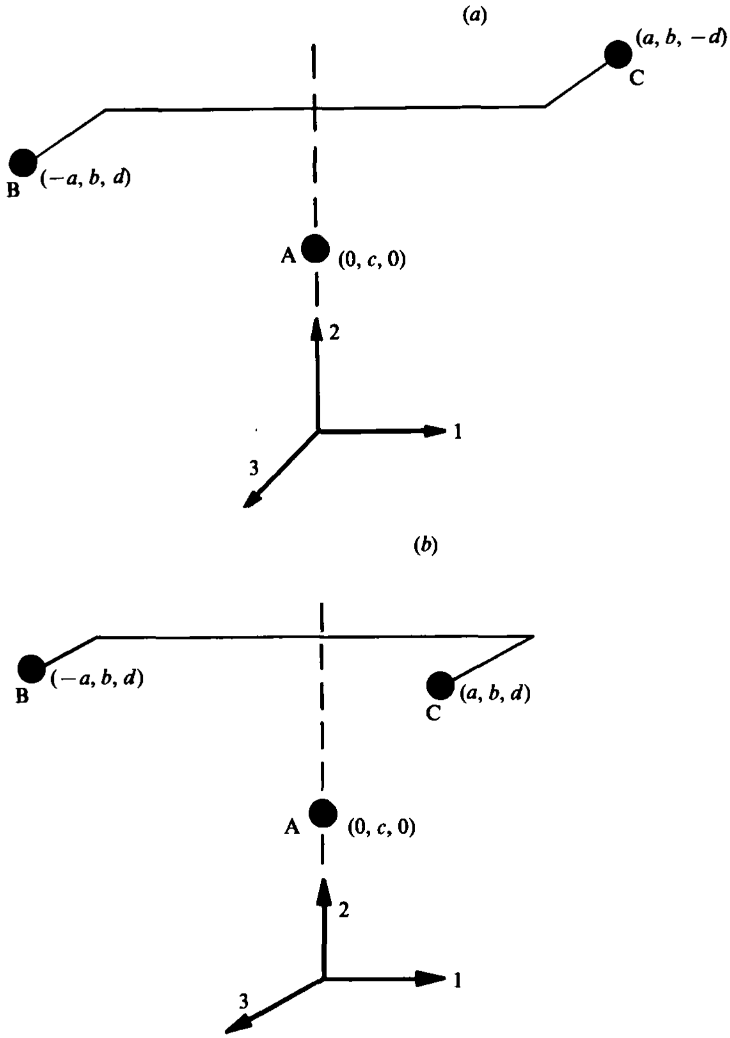

FIGURE 10. (a, b). Two kinds of fore–aft symmetry in three dimensions.

practice, at any particular moment there is not fore–aft symmetry in the duct, although in a time-averaged sense there is. This is substantiated by experiments (Goldsmith & Mason 1967) in which a dilute suspension of spheres was subjected to Couette flow. The motion of a single sphere was monitored as its experienced a succession of interaction events. While there were momentary lateral migrations these were small and furthermore there was no net migration. Net migrations occurred only in concentrated suspensions.

The previous discussion can be extended to include effects due to differences in y_3 position amongst the spheres. As long as the magnitude of the x_3 coordinate for B and C is the same (so that x is the same), the previous result holds (see figure 10). In practice we need only require fore–aft symmetry along every plane, of constant y_3 value, in the duct, to ensure that there are no lateral migrations.

While fore–aft symmetry causes cancellation of effects, an asymmetry may induce lateral migration and spreading down the duct. This can be seen in the experiment shown in figure 5. In practice spheres near the leading edge of a cloud of particles flowing down the duct will migrate laterally. Spheres near the trailing edge will also migrate. The configuration shown in figure 5 is not an arbitrary configuration. Under the influence of the inertially induced tubular-pinch effect, spheres will migrate to particular streamlines depending upon their size. Therefore there will be spheres on streamlines of like velocity on opposite sides of the centreline. This is the basis of inertially induced 'chromatography' (Altena & Belfort 1984). Therefore there will be lateral migrations of viscous origin occurring simultaneously with those of inertial origin. While the magnitude of the viscous migrations seems small it should be remembered that, at low Reynolds numbers, the order of magnitude of the viscous effect is much larger than the inertial effect by 1 to $1\frac{1}{2}$ orders. This phenomenon might impair such migration based separations as it has the effect of an enhanced axial diffusion coefficient.

In summary, as long as the spheres are not too close to the wall, and the Reynolds number is sufficiently small, first-order sphere–sphere interactions will be important only under situations of axial asymmetry in the distribution of spheres. In this case these interactions will be at least as important as inertially induced interactions.

This work was supported by the National Science Foundation under Grant Number CPE83-14443. Partial support of D.A.D. by the Mathematics Division of the U.S. Army Research Office under Contract DAAG29-85-G-0088 is acknowledged.

REFERENCES

ALTENA, F. W. & BELFORT, G. 1984 *Chem. Engng Sci.* **39**, 353.

BATCHELOR, G. K. 1976 In *Theoretical and Applied Mechanics* (ed. W. T. Koiter), p. 33 North Holland.

BRENNER, H. 1964 *Chem. Engng Sci.* **19**, 703.

BRETHERTON, F. P. 1964 *J. Fluid Mech.* **20**, 401.

COX, R. G. & BRENNER, H. 1967 *J. Fluid Mech.* **28**, 391.

COX, R. G. & BRENNER, H. 1968 *Chem. Engng Sci.* **23**, 147.

DREW, D. A. 1983 *Ann. Rev. Fluid Mech.* **15**, 261.

ECKSTEIN, E. C., BAILEY, D. G. & SHAPIRO, A. H. 1977 *J. Fluid Mech.* **79**, 193.

GOLDSMITH, H. L. & MASON, S. G. 1967 *Rheology, Theory and Applications* (ed. F. R. Eirich), Vol. 4 chap. 2, p. 176. Academic.

HO, B. P. & LEAL, L. G. 1974 *J. Fluid Mech.* **65**, 365.

HOCKING, L. M. 1964 *J. Fluid Mech.* **20**, 129.

ISHII, K. & HASIMOTO, H. 1980 *J. Phys. Soc. Japan* **48**, 2144.

KOGLIN, B. 1971 *Chem. Ing. Tech.* **43**, 761.

O'NEILL, M. E. 1981 *Sci. Prog. Oxf.* **67**, 149.

RUSSEL, W. B. 1981 *Ann. Rev. Fluid Mech.* **13**, 425.

SCHONBERG, J. A., DREW, D. A. & BELFORT, G. 1986 Transient interactions for two neutrally buoyant spheres in Poiseuille flow between two plates. *Chem. Engng Sci.* (submitted).

STOKES, G. G. 1851 *Trans. Camb. Phil. Soc.* **9**, 8.

VASSEUR, P. & COX, R. G. 1976 *J. Fluid Mech.* **78**, 385.